Many-body localization and thermalization in disordered Hubbard chains

Rubem Mondaini and Marcos Rigol

Phys. Rev. A **92**, 041601 — Published 6 October 2015

DOI: 10.1103/PhysRevA.92.041601

Many-body localization and thermalization in disordered Hubbard chains

Rubem Mondaini and Marcos Rigol
Department of Physics, The Pennsylvania State University, University Park, PA 16802, USA

We study the many-body localization transition in one-dimensional Hubbard chains using exact diagonalization and quantum chaos indicators. We also study dynamics in the delocalized (ergodic) and localized phases and discuss thermalization and eigenstate thermalization, or the lack thereof, in such systems. Consistently within the indicators and observables studied, we find that ergodicity is very robust against disorder, namely, even in the presence of weak Hubbard interactions the disorder strength needed for the system to localize is large. We show that this robustness might be hidden by finite size effects in experiments with ultracold fermions.

PACS numbers: 05.30.-d 67.85.-d, 71.30.+h

a. Introduction. Over the years, substantial attention has been devoted to understanding the dynamical properties of disordered systems. Interest on this topic goes back to a seminal paper by Anderson in 1958, who showed that sufficiently strong quenched disorder can produce localization of noninteracting particles, precluding transport in the thermodynamic limit [1]. Destructive interference is at the heart of this phenomenon. It is more prominent in lower dimensions, and, as a result, any nonzero disorder strength leads to localization in one and two dimensions [2]. A fundamental aspect of Anderson localization is that it occurs not only in the ground state but also in (highly) excited states.

Because of the possibility of localization occurring in interacting systems, a phenomenon termed many-body localization (MBL), disordered systems in the presence of interactions have received a lot of attention in recent years. Early perturbative arguments [3–6] and numerical simulations in the presence of strong interactions [7–11] have triggered much research on this topic [12, 13]. The MBL transition has also started to be explored in experiments with ultracold atoms [14–16] and ions [17].

The contrast between the properties of many-body eigenstates of interacting systems in the presence and absence of MBL makes apparent how remarkable MBL is. In generic isolated systems, interactions make possible for the system to act as its own 'effective bath'. If taken out of equilibrium, such systems evolve in time in such a way that observables equilibrate and can be described by traditional ensembles of statistical mechanics (i.e., they thermalize). This is just one of the manifestations of a phenomenon known as eigenstate thermalization [18–20], which, in short, means that the expectation value of an observable in an eigenstate of a many-body interacting system is the same as that in thermal equilibrium (with the same mean energy as the eigenstate energy). Eigenstate thermalization has been shown to occur in several many-body quantum systems [20–29]. It is known not to occur only in integrable and MBL systems, i.e., the latter two classes of systems generally do not exhibit thermalization even if they are thermodynamically large [30, 31].

As a matter of fact, it was the latter property of MBL systems the one used in the experiments of Ref. [15] to distinguish between the delocalized (ergodic) regime and the MBL one, for spinful fermions in the presence of a quasi-periodic potential. Motivated by those experiments, in this work we study the MBL transition in Hubbard chains with disorder. We contrast the predictions of quantum chaos indicators for the transition to those from thermalization and eigenstate thermalization. We argue that ergodicity is remarkably robust in these itinerant systems, and show that finite size effects in thermalization indicators might hide this fact in experiments.

b. Model and the MBL transition. To investigate the MBL transition, we use full exact diagonalization and study the Hamiltonian: $\hat{H} = \hat{H}_0 + \hat{H}_{\rm sb} + \hat{H}_W$, in which

$$\hat{H}_0 = -t \sum_{\substack{i=1 \\ \sigma=\uparrow,\downarrow}}^{L-1} (\hat{c}^\dagger_{i\sigma}\hat{c}_{i+1,\sigma} + \text{H.c.}) \\ -t' \sum_{\substack{i=1 \\ \sigma=\uparrow,\downarrow}}^{L-2} (\hat{c}^\dagger_{i\sigma}\hat{c}_{i+2,\sigma} + \text{H.c.}) + U \sum_{i}^{L} \hat{n}_{i\uparrow}\hat{n}_{i\downarrow}, \quad (1)$$

is an extended Hubbard model (written in standard notation) in a linear chain of size L (with open boundary conditions), with nearest neighbor hoppings (amplitude t), onsite interaction (strength U), and next-nearest neighbor hoppings (amplitude t'). We have taken $t' \neq 0$ so that the model is nonintegrable (quantum chaotic) in the absence of disorder. Additional symmetries, parity and $SU(2)$, are removed by adding a very weak magnetic field (h_b) and chemical potential (μ_b), respectively, at the opposite edges of the chain: $\hat{H}_{\rm sb} = h_b(\hat{n}_{1,\uparrow} - \hat{n}_{1,\downarrow}) + \mu_b(\hat{n}_{L,\uparrow} + \hat{n}_{L,\downarrow})$ (see Ref. [32] for details). We focus on a uniformly distributed disorder described by $\hat{H}_W = \sum_{i\sigma} \varepsilon_i \hat{n}_{i\sigma}$, where the local potential $\varepsilon_i \in [-W/2, W/2]$. To show the stark contrast between disorder and the quasi-periodic potential studied in Refs. [15], we also report results for the phase diagram when $\varepsilon_i = \frac{\Delta}{2}\cos(2\pi\beta i + \phi)$, where Δ is the potential strength, $\beta = (\sqrt{5}+1)/2$ is the golden ratio, and ϕ is an arbitrary phase (as in the Aubry-Andre model [33]). Throughout this manuscript, $t = 1$ sets the energy scale and $t' = 0.5$. We only change U and the disorder strength. The systems studies are at quarter

filling, namely, $N_\uparrow + N_\downarrow = L/2$, with $N_\uparrow \equiv \langle \sum_i^L \hat{n}_{i\uparrow} \rangle$ and $N_\downarrow \equiv \langle \sum_i^L \hat{n}_{i\downarrow} \rangle$. We consider two lattice sizes, $L = 10$ and 12, where $N_\uparrow = N_\downarrow = L/4$ for $L = 12$, and $N_\uparrow = N_\downarrow \pm 1$ for $L = 10$ [32].

A common quantum chaos indicator used to locate the many-body localization transition in disordered systems is the average ratio between the smallest and the largest adjacent energy gaps, $r_n = \min[\delta_n^E, \delta_{n-1}^E]/\max[\delta_n^E, \delta_{n-1}^E]$, with $\delta_n^E = E_n - E_{n-1}$, and $\{E_n\}$ is the ordered list of energy levels [7]. Here, in order to reduce finite size effects, we compute the average ratio $\bar{r}$ over the central half of the spectrum. In the ergodic phase, when the level spacing exhibits a Wigner-Dyson distribution, the average ratio is $r^{\rm WD} \approx 0.536$, while in the MBL phase, when the level spacing exhibits a Poisson distribution, the average ratio is $r^{\rm P} = 2\ln 2 - 1 \approx 0.386$ [34].

Figure 1 shows the disorder average of $\bar{r}$, $\langle \bar{r} \rangle_{\rm dis}$, as a function of the disorder strength for different values of the on-site repulsion and two system sizes. The value of the disorder strength at which the curves cross/merge, W_c, can be taken as an estimate of the critical disorder strength for the ergodic to many-body localization phase transition. Such a crossing/merging point is known to move towards stronger disorder with increasing system size (see, e.g., Refs. [7, 9, 10]), as such, the values reported here should be thought of as lower bounds for the critical disorder. As expected, since interactions promote delocalization, W_c first increases with U [Figs. 1(a)–1(c)]. It is remarkable that, even for fairly small values of U [$U = 0.2$ in Fig. 1(a)], the delocalized regime is robust up to values of $W_c \simeq 8$, i.e., almost twice the width B of the single particle spectrum, $\epsilon_k = -2t\cos(k) - 2t'\cos(2k)$ ($B = 4.5$ for our parameters). As the onsite interaction strength becomes of the order of B, W_c stops increasing and, as U increases further, W_c starts to decrease [Figs. 1(c) and 1(d)]. This is expected as, in the limit $U \to \infty$, each sector in the Hubbard model with a particular ordering of the spins (and no double occupancy) maps onto a *noninteracting* spinless fermion Hamiltonian with $N_\uparrow + N_\downarrow$ fermions, and the latter localizes for any nonzero disorder strength. Figure 1(e) depicts the estimated phase diagram in the presence of disorder for up to $U = 20$. In contrast, as also shown in Fig. 1(e), MBL in the present of a quasi-periodic potential (see Ref. [32] for further details) occurs for $\Delta \ll W$. MBL is also easier to achieve in interacting spinless fermion systems [35].

c. Dynamics and thermalization. As mentioned before, one of the defining properties of the MBL phase is its lack of thermalization. In what follows, motivated by the experimental results reported in Ref. [15], we study dynamics in the delocalized and MBL regimes. Our initial state is also experimentally motivated. We consider $|\psi_I\rangle = |\uparrow 0 \downarrow 0 \uparrow 0 \downarrow \ldots\rangle$, which is a state that has no double occupancy and can be prepared using optical superlattices. $|\psi_I\rangle$ is a quarter-filling version of the state prepared in Ref. [15]. The dynamics is then studied under $\hat{H} = \hat{H}_0 + \hat{H}_{\rm sb} + \hat{H}_W$. Our goal is to understand how the results of the dynamics relate to those obtained for

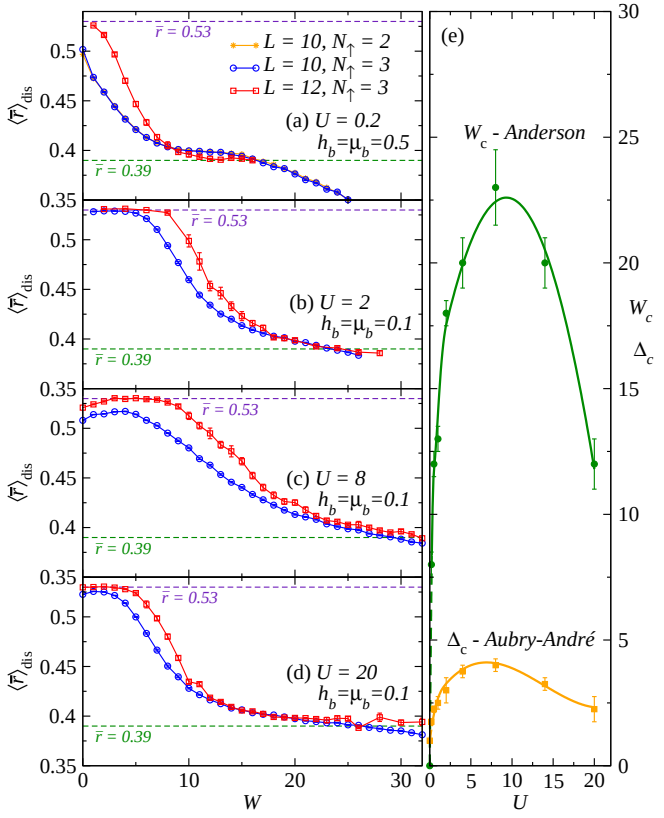

FIG. 1. (Color online) (a)-(d) Averaged ratio of adjacent energy gaps as a function of the disorder strength for four values of U and two lattice sizes. The average $\bar{r}$ was computed over the central half of the spectrum. The disordered averaged results $\langle \bar{r} \rangle_{\rm dis}$ for $L = 10$ were obtained averaging over 1200 disorder realizations, and the ones for $L = 12$ over 20–200 disorder realizations (error-bars report the standard deviation). In (a), we show results for $N_\uparrow = N_\downarrow \pm 1$ when $L = 10$. They make apparent that both sectors behave qualitative (and quantitatively) similarly even for the largest values of $h_b = \mu_b$ used. The crossing point between curves for different lattice sizes provides an estimate of the critical disorder, W_c, for the ergodic to MBL transition. (e) Estimated W_c and Δ_c as a function of U (error-bars report an interval of confidence based on the closeness of the results about W_c).

$\bar{r}$. Some of the specific questions we address are: Is the MBL transition manifest in the dynamics of experimentally relevant observables? At which time those observables reach (if they do) stationary values? We are also interested in understanding the role of finite size effects. They have been found to be stronger in indicators related to Hamiltonian eigenstates than in those related to the spectrum [36]. To address these questions, we focus in one particular value of the interaction strength, $U = 4$.

We report results for three observables (see Ref. [32] for another one). Two observables, *the imbalance* $I = (\langle \hat{n}^e \rangle - \langle \hat{n}^o \rangle)/(\langle \hat{n}^e \rangle + \langle \hat{n}^o \rangle)$, where $\hat{n}^{e(o)} = \sum_{i={\rm even(odd)},\sigma} \hat{n}_{i,\sigma}$ (I was measured in Ref. [15]), and the kinetic energy $K = -t\sum_{i,\sigma}\langle(\hat{c}_{i\sigma}^\dagger \hat{c}_{i+1,\sigma} + {\rm H.c.})\rangle - t'\sum_{i,\sigma}\langle(\hat{c}_{i\sigma}^\dagger \hat{c}_{i+2,\sigma} + {\rm H.c.})\rangle$,

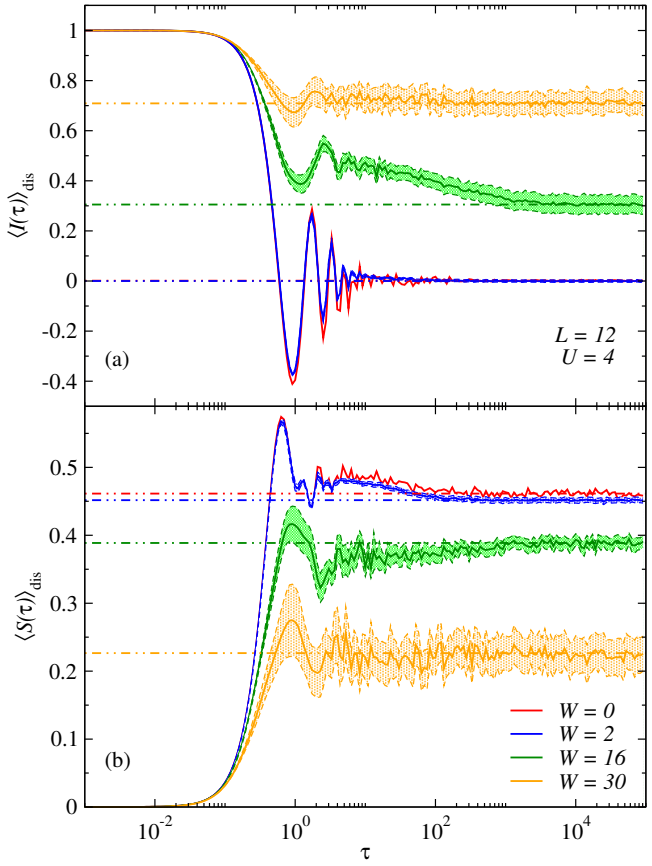

FIG. 2. (Color online) Disorder averaged results for the time evolution of: (a) the even-odd site occupation imbalance, and (b) the antiferromagnetic structure factor. The shaded area around the curves depicts the standard deviation of the mean, after an average over 10 disorder realizations. The horizontal dashed lines depict the disorder averaged values of the diagonal ensemble predictions (see text).

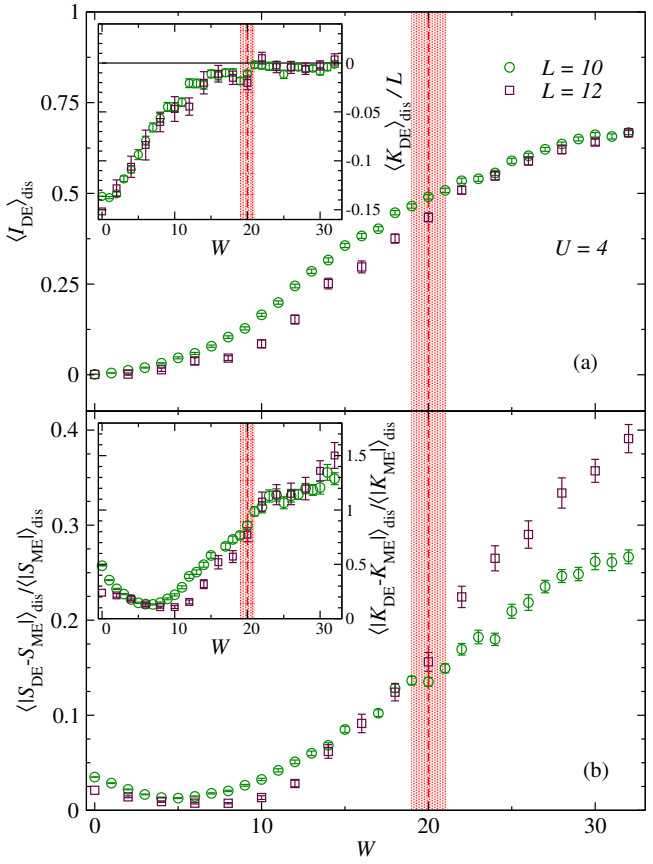

FIG. 3. (Color online) (a) Disorder averaged diagonal ensemble results for the imbalance (main panel) and the kinetic energy per site (inset) vs the amplitude of the disorder W. (b) Normalized disorder average difference between the diagonal and microcanonical ensemble predictions for the structure factor (main panel) and the kinetic energy (inset) vs the amplitude of the disorder W. In all cases $U = 4$, and the width of the microcanonical energy window is $\Delta E = 0.1$. The vertical dashed line marks W_c, and the shaded region around it signals the interval of confidence reported in Fig. 1(e).

are directly related to the charge degrees of freedom. The third one, the antiferromagnetic structure factor $S = 1/L \sum_{i,j} e^{i\pi(i-j)} \langle (\hat{n}_{i\uparrow} - \hat{n}_{i\downarrow})(\hat{n}_{j\uparrow} - \hat{n}_{j\downarrow}) \rangle$ is related to the spin degrees of freedom (from now on we refer to it as *the structure factor*). The relaxation times of the charge and spin degrees of freedom are expected to be different for very strong interactions [37].

Figure 2 displays the disorder averaged time evolution of the imbalance [Fig. 2(a)] and of the structure factor [Fig. 2(b)]. We also display, as horizontal dashed lines, the disorder average of the diagonal ensemble results. Given an observable $\widehat{\mathcal{O}}$, the diagonal ensemble result (which, in the absence of degeneracies, is the same as the infinite-time average of the observable [20]) can be obtained as $\mathcal{O}_{\rm DE} = \sum_\alpha |C_\alpha|^2 \mathcal{O}_{\alpha\alpha}$, where $\mathcal{O}_{\alpha\alpha} = \langle \alpha | \widehat{\mathcal{O}} | \alpha \rangle$, $|\alpha\rangle$ are the eigenstates of the Hamiltonian ($\hat{H}|\alpha\rangle = E_\alpha |\alpha\rangle$, E_α are the eigenenergies), and $C_\alpha = \langle \alpha | \psi_I \rangle$. We say that $\widehat{\mathcal{O}}$ equilibrates if it relaxes to $\mathcal{O}_{\rm DE}$ and remains close to it for long time.

Figures 2(a) and 2(b) show that I and S equilibrate in both the delocalized and localized regimes. Sufficiently far away from W_c ($W = 0$, 2, and 30 in the figure), one can see that both observables have essentially reached the diagonal ensemble result (or are very close to it) for $\tau \simeq 10\,(\hbar/t)$. As the system approaches $W_c (\simeq 20$ for $U = 4$), we find that equilibration times become much longer. For example, for $W = 16$ in Fig. 1(a), one can see that I becomes nearly time independent only at $\tau \simeq 10^3\,(\hbar/t)$. Very long equilibration times at a delocalization to localization transition have also been observed, for much larger system sizes, in the integrable hard-core boson version of the Aubry-André model [38]. Those times represent a challenge for experiments.

Next, we check how the diagonal ensemble results for the observables compare to the microcanonical predictions. Whenever they agree, and equilibration occurs (as we have checked), we say that the system thermalizes. We first consider I. Since there is no distinction between

even and odd sites in the Hamiltonian, the disorder average of I is expected to be zero in the microcanonical ensemble ($\langle I_{\rm ME}\rangle_{\rm dis} = 0$). Hence, as argued in Ref. [15], the disorder average of the diagonal ensemble result for I ($\langle I_{\rm DE}\rangle_{\rm dis}$) can be taken to be the order parameter for the MBL phase (it can only differ from zero if the system does not thermalize). Figure 3(a) shows $\langle I_{\rm DE}\rangle_{\rm dis}$ vs W for two system sizes. For the (small) system sizes that we can study, $\langle I_{\rm DE}\rangle_{\rm dis}$ can be seen to smoothly increase from zero with increasing W. However, comparing the results for the two system sizes, one can see that in the delocalized side (and close to W_c in the MBL side) $\langle I_{\rm DE}\rangle_{\rm dis}$ decreases with increasing system size. This is consistent with the expectation that, in the thermodynamic limit, it will vanish in the delocalized side.

Another order parameter that could be used to locate the MBL transition in experiments is the kinetic energy. As discussed in Ref. [31], the dynamics of one-particle corrections in the MBL phase is quantitatively similar to that in the atomic limit (even if the system is not in that limit). This means that, in the Heisenberg representation, $\hat{c}^\dagger_{i,\sigma}(\tau)\hat{c}_{j,\sigma}(\tau) \approx \exp[i(\varepsilon_i - \varepsilon_j)\tau/\hbar]\hat{c}^\dagger_{i,\sigma}(0)\hat{c}_{j,\sigma}(0)$. Given our initial state, that implies that $\langle K_{\rm DE}\rangle_{\rm dis} \approx 0$. In the inset in Fig. 3(a), one can see that, indeed, $\langle K_{\rm DE}\rangle_{\rm dis} \approx 0$ for $W \gtrsim W_c$. In Fig. 3(b), the inset shows $\langle |K_{\rm DE} - K_{\rm ME}|\rangle_{\rm dis}/\langle |K_{\rm ME}|\rangle_{\rm dis}$ and the main panel shows $\langle |S_{\rm DE} - S_{\rm ME}|\rangle_{\rm dis}/\langle |S_{\rm ME}|\rangle_{\rm dis}$. Both normalized differences can be seen to decrease with increasing system size in the delocalized phase and not in the MBL. This is consistent with the expectation that thermalization occurs only in the former.

The fact that the system thermalizes (fails to thermalize) in the delocalized (MBL) regime can be understood to be the result of eigenstate thermalization occurring (not occurring) in that regime [18–20]. In Fig. 4, we show the eigenstate expectation values of the three observables of interest for a single disorder realization for different values of W. Deep in the delocalized phase ($W = 0$ and 2 in the figure), the support for those expectation values at a given energy can be seen to be very small (it decreases with system size, not shown), i.e., eigenstate thermalization occurs. The support of the eigenstate expectation values exhibits a different behavior within the MBL phase, or close to it, ($W = 16$ and 30 in the figure), i.e., eigenstate thermalization does not occur, or, at least, it is not apparent for the system sizes studied. In Fig. 4, vertical dashed lines depict the mean energy, and shaded areas around them depict the width of the energy distribution (for $W = 0$ and 2), in the quenches involving that disorder realization. They show which part of the spectrum is relevant to the dynamics studied.

d. Summary and discussion. We have studied the ergodic to MBL transition in Hubbard chains. Our main result from the analysis of quantum chaos indicators is that ergodicity is very robust against disorder. Even for on-site interactions as weak as $U = 0.2$, we find that the disorder strength required to localize the system is or the order of twice the single-particle bandwidth. We

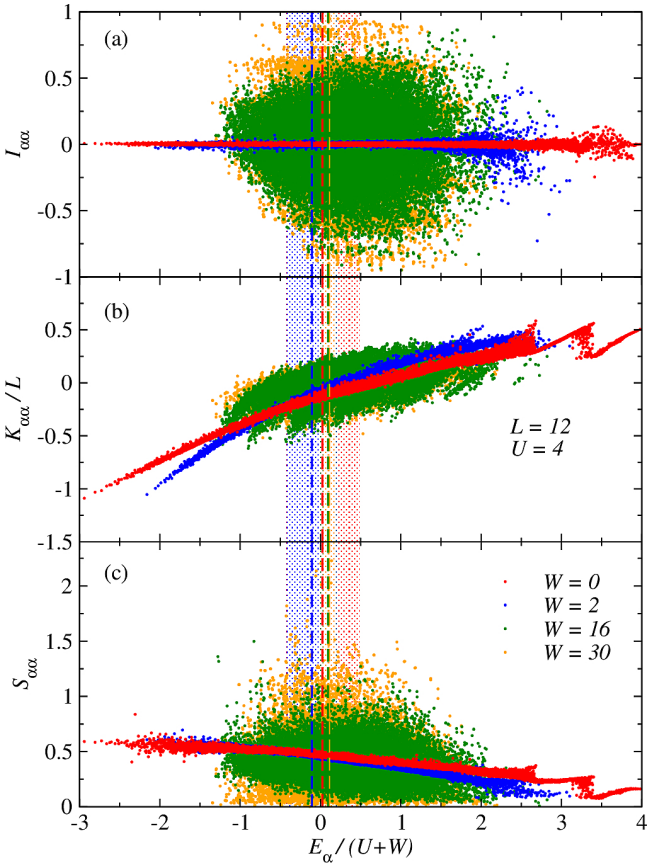

FIG. 4. (Color online) Eigenstate expectation values of the imbalance (a), the kinetic energy per site (b), and the structure factor (c) for a single disorder realization in systems with four different disorder strengths. The vertical dashed lines show the averaged mean energy, and the shaded are for $W = 0$ and 2 depict the averaged energy width, for the quenches involving this disorder realization. The results reported here were obtained in systems with $U = 4$ and $L = 12$.

studied the dynamics of those systems starting from a state of the form $|\psi_I\rangle = |\uparrow 0 \downarrow 0 \uparrow 0 \downarrow \ldots\rangle$. We find that various experimentally relevant observables equilibrate in time scales $\sim 1-10(\hbar/t)$, whenever the system is not close to the MBL transition. Close to the MBL transition, equilibration times become orders of magnitude longer and might be difficult to handle experimentally. We have also studied the differences between observables after equilibration and the predictions of the microcanonical ensemble finding that, for the small lattice sizes that we are able to study (~ 12 sites), they increase smoothly as one increases disorder and can be large even far from the MBL transition. This is reminiscent of the behavior observed as one approaches an integrable point in finite systems [21, 22]. Hence, the analysis of a few small system sizes does not allow one to identify the critical disorder strength at which MBL occurs. Large system sizes, or a careful finite size scaling analysis, are needed. While that might be possible in experiments, it remains a challenge for numerical simulations. Numerical linked cluster

expansions [30, 31], which exhibit an exponentially fast convergence with increasing the size of the systems that need to be diagonalized [39], offer a promising way to address this challenge [31].

e. Acknowledgments This work was supported by the National Science Foundation Grant No. PHY13-18303, the US Army Research Office, and CNPq (R.M.). The computations were performed in the Institute for CyberScience at Penn State, the Center for High-Performance Computing at the University of Southern California, and CENAPAD-SP.

[1] P. W. Anderson, "Absence of diffusion in certain random lattices," Phys. Rev. **109**, 1492 (1958).
[2] E. Abrahams, P. W. Anderson, D. C. Licciardello, and T. V. Ramakrishnan, "Scaling theory of localization: Absence of quantum diffusion in two dimensions," Phys. Rev. Lett. **42**, 673–676 (1979).
[3] L. Fleishman and P. W. Anderson, "Interactions and the Anderson transition," Phys. Rev. B **21**, 2366–2377 (1980).
[4] B. L. Altshuler, Y. Gefen, A. Kamenev, and L. S. Levitov, "Quasiparticle lifetime in a finite system: A nonperturbative approach," Phys. Rev. Lett. **78**, 2803–2806 (1997).
[5] I. V. Gornyi, A. D. Mirlin, and D. G. Polyakov, "Interacting electrons in disordered wires: Anderson localization and low-T transport," Phys. Rev. Lett. **95**, 206603 (2005).
[6] D. M. Basko, I. L. Aleiner, and B. L. Altshuler, "Metalinsulator transition in a weakly interacting many-electron system with localized single-particle states," Ann. Phys. **321**, 1126 – 1205 (2006).
[7] V. Oganesyan and D. A. Huse, "Localization of interacting fermions at high temperature," Phys. Rev. B **75**, 155111 (2007).
[8] M. Žnidarič, T. Prosen, and P. Prelovšek, "Many-body localization in the heisenberg XXZ magnet in a random field," Phys. Rev. B **77**, 064426 (2008).
[9] A. Pal and D. A. Huse, "Many-body localization phase transition," Phys. Rev. B **82**, 174411 (2010).
[10] E. Khatami, M. Rigol, A. Relaño, and A. M. Garcia-Garcia, "Quantum quenches in disordered systems: Approach to thermal equilibrium without a typical relaxation time," Phys. Rev. E **85**, 050102(R) (2012).
[11] J. H. Bardarson, F. Pollmann, and J. E. Moore, "Unbounded growth of entanglement in models of many-body localization," Phys. Rev. Lett. **109**, 017202 (2012).
[12] R. Nandkishore and D. A. Huse, "Many-body localization and thermalization in quantum statistical mechanics," Annual Review of Condensed Matter Physics **6**, 15–38 (2015).
[13] E. Altman and R. Vosk, "Universal dynamics and renormalization in many-body-localized systems," Annual Review of Condensed Matter Physics **6**, 383–409 (2015).
[14] S. S. Kondov, W. R. McGehee, W. Xu, and B. DeMarco, "Disorder-induced localization in a strongly correlated atomic Hubbard gas," Phys. Rev. Lett. **114**, 083002 (2015).
[15] M. Schreiber, S. S. Hodgman, P. Bordia, H. P. Lüschen, M. H. Fischer, R. Vosk, E. Altman, U. Schneider, and I. Bloch, "Observation of many-body localization of interacting fermions in a quasi-random optical lattice," arXiv:1501.05661 (2015).
[16] Pranjal Bordia, Henrik P Lüschen, Sean S Hodgman, Michael Schreiber, Immanuel Bloch, and Ulrich Schneider, "Coupling identical 1d many-body localized systems," arXiv preprint arXiv:1509.00478 (2015).
[17] Jacob Smith, Aaron Lee, Philip Richerme, Brian Neyenhuis, Paul W Hess, Philipp Hauke, Markus Heyl, David A Huse, and Christopher Monroe, "Many-body localization in a quantum simulator with programmable random disorder," arXiv preprint arXiv:1508.07026 (2015).
[18] J. M. Deutsch, "Quantum statistical mechanics in a closed system," Phys. Rev. A **43**, 2046 (1991).
[19] M. Srednicki, "Chaos and quantum thermalization," Physical Review E **50**, 888 (1994).
[20] M. Rigol, V. Dunjko, and M. Olshanii, "Thermalization and its mechanism for generic isolated quantum systems," Nature **452**, 854–858 (2008).
[21] M. Rigol, "Breakdown of thermalization in finite one-dimensional systems," Phys. Rev. Lett. **103**, 100403 (2009).
[22] M. Rigol, "Quantum quenches and thermalization in one-dimensional fermionic systems," Phys. Rev. A **80**, 053607 (2009).
[23] L. F. Santos and M. Rigol, "Localization and the effects of symmetries in the thermalization properties of one-dimensional quantum systems," Phys. Rev. E **82**, 031130 (2010).
[24] C. Neuenhahn and F. Marquardt, "Thermalization of interacting fermions and delocalization in Fock space," Phys. Rev. E **85**, 060101 (2012).
[25] E. Khatami, G. Pupillo, M. Srednicki, and M. Rigol, "Fluctuation-dissipation theorem in an isolated system of quantum dipolar bosons after a quench," Phys. Rev. Lett. **111**, 050403 (2013).
[26] R. Steinigeweg, J. Herbrych, and P. Prelovšek, "Eigenstate thermalization within isolated spin-chain systems," Phys. Rev. E **87**, 012118 (2013).
[27] W. Beugeling, R. Moessner, and Masudul Haque, "Finite-size scaling of eigenstate thermalization," Phys. Rev. E **89**, 042112 (2014).
[28] H. Kim, T. N. Ikeda, and D. A. Huse, "Testing whether all eigenstates obey the eigenstate thermalization hypothesis," Phys. Rev. E **90**, 052105 (2014).
[29] S. Sorg, L. Vidmar, L. Pollet, and F. Heidrich-Meisner, "Relaxation and thermalization in the one-dimensional Bose-Hubbard model: A case study for the interaction quantum quench from the atomic limit," Phys. Rev. A **90**, 033606 (2014).
[30] M. Rigol, "Quantum quenches in the thermodynamic limit," Phys. Rev. Lett. **112**, 170601 (2014).
[31] B. Tang, D. Iyer, and M. Rigol, "Quantum quenches and many-body localization in the thermodynamic limit," Phys. Rev. B **91**, 161109(R) (2015).

[32] See Supplemental Material for more information about the weak symmetry breaking fields, quantum chaos indicators, and observables.
[33] Serge Aubry and Gilles André, "Analyticity breaking and anderson localization in incommensurate lattices," Ann. Israel Phys. Soc **3**, 18 (1980).
[34] Y. Y. Atas, E. Bogomolny, O. Giraud, and G. Roux, "Distribution of the ratio of consecutive level spacings in random matrix ensembles," Phys. Rev. Lett. **110**, 084101 (2013).
[35] This reentrant behavior in the localized phase was also observed in a related model with spinless fermions: Y. Bar Lev, G. Cohen, and David R. Reichman, "Absence of diffusion in an interacting system of spinless fermions on a one-dimensional disordered lattice," Phys. Rev. Lett. **114**, 100601 (2015).
[36] L. F. Santos and M. Rigol, "Onset of quantum chaos in one-dimensional bosonic and fermionic systems and its relation to thermalization," Phys. Rev. E **81**, 036206 (2010).
[37] A. Bauer, F. Dorfner, and F. Heidrich-Meisner, "Temporal decay of Néel order in the one-dimensional Fermi-Hubbard model," Phys. Rev. A **91**, 053628 (2015).
[38] C. Gramsch and M. Rigol, "Quenches in a quasidisordered integrable lattice system: Dynamics and statistical description of observables after relaxation," Phys. Rev. A **86**, 053615 (2012).
[39] D. Iyer, M. Srednicki, and M. Rigol, "Optimization of finite-size errors in finite-temperature calculations of unordered phases," Phys. Rev. E **91**, 062142 (2015).